Khdc3 Regulates Metabolism Across Generations in a DNA-Independent Manner

Liana Senaldi[1,2], Nora Hassan[1], Sean Cullen[1,2], Uthra Balaji[2], Natalie Trigg[3], Jinghua Gu[2], Hailey Finkelstein[1], Kathryn Phillips[1], Colin Conine[3], Matthew Smith-Raska[1,2]

1. Division of Neonatology, Department of Pediatrics, Weill Cornell Medicine, New York-Presbyterian Hospital, New York, NY, USA.
2. Drukier Institute for Children's Health, Weill Cornell Medicine, New York, NY, USA. mrs7001@med.cornell.edu.
3. Departments of Genetics and Paediatrics, University of Pennsylvania Perelman School of Medicine and Children's Hospital of Philadelphia, Philadelphia, PA, USA.

Abstract

Genetic variants can alter the profile of heritable molecules such as small RNAs in sperm and oocytes, and in this manner ancestral genetic variants can have a significant effect on offspring phenotypes even if they are not inherited. Here we show that wild type female mice descended from ancestors with a mutation in the mammalian germ cell gene *Khdc3* have hepatic metabolic defects that persist over multiple generations. We find that genetically wild type females descended from *Khdc3* mutants have transcriptional dysregulation of critical hepatic metabolic genes, which persist over multiple generations and pass through both female and male lineages. This was associated with dysregulation of hepatically-metabolized molecules in the blood of these wild type mice with mutational ancestry. The oocytes of *Khdc3*-null females, as well as their wild type descendants, had dysregulation of multiple small RNAs, suggesting that these epigenetic changes in the gametes transmit the phenotype between generations. Furthermore, injection of serum from wild type mice with ancestral history of *Khdc3* mutation into wild type females is sufficient to cause hepatic transcriptional dysregulation in their offspring. Our results demonstrate that ancestral mutation in *Khdc3* can produce transgenerational inherited phenotypes, potentially indefinitely.

47 **Introduction**

48 It is becoming increasingly apparent that non-DNA molecules inherited from germ cells contribute
49 significantly to the transmission of traits and diseases across generations. This has been
50 demonstrated in response to a variety of exposures such as diet or stress in model organisms (1, 2)
51 and has been confirmed in human epidemiological studies (3, 4). The mechanisms driving this
52 process remain poorly defined and are complicated by the erasure of acquired epigenetic molecules
53 such as DNA methylation early in embryonic development. Expression of germ cell small RNAs
54 such as microRNA (miRNA) and tRNA fragments (tsRNA) are responsive to exposures and
55 inherited at fertilization, making them potential candidates for passage of phenotypic information
56 across generations (1, 5). Microinjection of these small RNAs from the germ cells of an exposed
57 mouse into an unexposed embryo is sufficient to recapitulate the descendant's phenotypes,
58 demonstrating causality (1). However, the absence of an RNA-dependent RNA polymerase in
59 mammals suggests that small RNAs by themselves cannot propagate phenotypes across multiple
60 generations.

61

62 Non-inherited ancestral genetic variants can also affect descendants' risk of disease, as has been
63 demonstrated in cancer (6, 7), thyroid hormone metabolism (8), body weight (9), anxiety (10), type
64 I diabetes (11), and folate metabolism (12). This phenomenon is often referred to as "genetic
65 nurture" based on the effect of non-inherited DNA variants nurturing phenotypes in the next
66 generation (13). In all described cases, the observed phenotypes disappear after a few generations.
67 The molecular mechanisms driving these cross-generational traits, in the absence of inheritance of
68 the causal variant, remains largely undescribed, with the exception of paramutation effects that are
69 driven by inherited RNA molecules (14, 15). Some of the genes associated with genetic nurture

70 act by altering the expression of RNAs in the gamete, which can affect processes such as glucose
71 metabolism and body weight (16). Other reported examples involve genes that do not have any
72 known function in the germ cells, and likely alter descendants' phenotypes indirectly, by changing
73 underlying physiology in a manner that subsequently alters germ cell heritable molecules, not
74 dissimilar from the mechanisms of exposure-based changes to heritable germ cell molecules (8).
75
76 These experiments are typically performed in males to avoid the confounding influence of in utero-
77 and breastmilk-mediated effects. As a result, examination of oocyte small RNAs in the inheritance
78 of phenotypes has been much less studied, because of the confounding influence of the placenta
79 and breastmilk, and also because the dozens of oocytes per mouse yield much less RNA than can
80 be obtained from the millions of sperm isolated from a male. However, in vitro fertilization has
81 been utilized to demonstrate that oocytes are also capable of transmitting exposure-based non-
82 genetic information across generations (17).
83
84 *Khdc3* is a mammalian gene expressed in the male and female germ cells that encodes a protein
85 containing an RNA-binding KH domain that localizes to a multi-protein complex at the oocyte
86 periphery known as the subcortical maternal complex (18, 19). *Khdc3*-null female mice have
87 decreased fertility caused by defects in maintaining euploidy during embryogenesis (20). Human
88 females with homozygous mutations in the ortholog *KHDC3L* are infertile, which has been
89 associated with abnormal DNA methylation in oocytes (18). *KHDC3L* (and *Khdc3)* does not
90 localize to the nucleus and does not contain a DNA methyltransferase domain, suggesting that the
91 DNA methylation defects are secondary outcome and not the main function of this gene.
92

93 We demonstrate that wild type female descendants of *Khdc3*-null mice have dysfunctional
94 expression of hepatic metabolic genes that persists over multiple generations, and that this effect
95 is transmitted from both male and female mutant ancestors. This corresponds with abnormal levels
96 of hepatic metabolites in the serum of these wild type mice with mutant ancestors. The persistence
97 of these abnormalities in genetically wild type mice suggests that altered epigenetic information
98 in the germ cells is transmitting the inherited metabolic phenotypes. Accordingly, we observed
99 that the oocytes of *Khdc3*-null females and their wild type descendants have multiple dysregulated
100 miRNAs and tsRNAs, suggesting a mechanism of inheritance.
101
102 **Results**
103 *Wild type females descended from Khdc3-null ancestors display hepatic transcriptional*
104 *dysregulation.*
105 Global transcriptome analysis of *Khdc3*-null oocytes revealed significant dysregulation of genes
106 important in metabolic processes regulated by the liver, especially the metabolism of lipids
107 (atherosclerosis, PPAR signaling, and pantothenate and CoA metabolism) and of carbohydrates
108 (glycolysis/gluconeogenesis, and fructose and mannose metabolism) (Fig. 1A) (21-24). Despite
109 the abnormal expression of metabolic genes in the *Khdc3*-null oocyte, this gene is only expressed
110 in female reproductive tissue, with no detectable expression in the liver and minimal expression in
111 other metabolic tissues such as adipose or pancreas (Fig. 1B).
112
113 Expression of *Cyp17a1*, a gene central to lipid metabolism (25, 26), was increased in the livers of
114 *Khdc3*-null (knockout, or "KO") females, despite a lack of expression or any known function of
115 *Khdc3* in wild type livers. Elevated expression of *Cyp17a1* was observed in KO females generated

116 from KO parents (referred to as "KO^{KO}") as well as KO females generated by mating *Khdc3*
117 heterozygote parents (referred to as "KO*") (Fig. 1C). *Cyp17a1* expression was also significantly
118 increased, to the same extent as KO^{KO} and KO* females, in genetically wild type females
119 descended from heterozygous parents (referred to as "WT*" to indicate genetically wild type mice
120 that have descended from *Khdc3* heterozygous mutant parents and a combination of wild type and
121 *Khdc3*-null grandparents). Thus, having an ancestor that carried a *Khdc3* mutation was associated
122 with elevated *Cyp17a1* expression, and the *Khdc3* genotype had no effect on *Cyp17a1* expression,
123 revealing a DNA-independent form of inheritance (Fig. 1C). Increased *Cyp17a1* mRNA
124 expression was observed in WT* females generated from all possible combinations of male and
125 female KO grandparents (Fig. 1D). In addition to conventional genotyping, the wild type genotype
126 of these mice was confirmed with RNA-Seq of ovaries (Supplemental Figure 1).
127
128 RNA-Seq of female WT* livers revealed a pattern of global transcriptional dysregulation that
129 overlapped significantly with KO* and KO^{KO} females (Fig. 1E-F), demonstrating that shared
130 ancestry rather than genotype accounts for the transcriptional abnormalities in WT* mice. This is
131 supported by the observation that most significantly dysregulated genes in WT* livers were
132 similarly dysregulated in KO* livers (Fig. 1G). Gene ontology of the common dysregulated genes
133 in livers of WT* and KO* mice revealed enrichment in metabolic processes in which the liver
134 plays a central role, especially lipid and glucose metabolism (24-27) (Fig. 1H).
135
136 *WT* defects persist over multiple generations.*
137 When WT* male and female mice were mated with each other to generate the next generation
138 (referred to as WT**, signifying the 2nd generation of genetically wild type mice), hepatic

139 transcriptional dysregulation of metabolic genes persisted. There was a similar pattern of
140 dysregulation in WT** females derived from either male or female *Khdc3*-null ancestors (denoted
141 WT**(P) and WT**(M), respectively, denoting Paternal or Maternal ancestral mutant history)
142 (Fig. 2A-B). Comparison of dysregulated genes between WT**(P) and WT**(M) females showed
143 significant overlap (Fig. 2C) revealing that the same pattern of abnormal gene expression is
144 observed in wild type females descended from both male and female mutant ancestors.
145
146 WT(P) male and female mice were mated with each other in order to examine passage these defects
147 over successive generations. Descendants of male mutants were examined to avoid potential
148 confounding from non-germ cell mechanisms of inheritance such as mitochondrial inheritance,
149 fetal-maternal communication across the placenta, or transmission of molecules via breastmilk.
150 Expression of *Cyp17a1* and *2610507I01Rik*, two genes dysregulated in WT*, KO*, KO^{KO}, and
151 WT**(P) female mice, demonstrated persistent and worsening dysregulated expression in the 2nd
152 through 6th generation of females, in which each additional asterisk (*) denotes the successive
153 number of genetically wild type generations (Fig. 2D). In a minority of mice, expression reverted
154 back to WT levels (Fig. 2D). Importantly, those mice that reverted to wild type levels of *Cyp17a1*
155 maintained elevated expression of *2610507I01Rik*, and vice-versa, suggesting that the abnormal
156 expression of these genes is driven by independent units of inheritance.
157
158 *Khdc3*-null females were outcrossed with a true wild type male without any ancestral history of
159 *Khdc3* mutation, in order to examine the persistence of the observed defects through only the
160 maternal line without any contribution from males that descended from mutants. 100% of the F2
161 outcrossed females, descended from a maternal grandmother mutant, had persistent transcriptional

162 dysregulation of metabolism-related genes in the liver (Fig. 2E). Many of these dysregulated genes
163 overlapped with WT* females descended from both male (WT*(P)) and female (WT*(M))
164 homozygous-null ancestors (Fig 2F). In this mating scheme, persistence of hepatic transcriptional
165 dysregulation in all 7 examined females is not consistent with mechanisms of inheritance involving
166 in-cis transmission, including an unaccounted DNA polymorphism/mutation, DNA methylation,
167 or histone protein modification, in which any chromosome from the *Khdc3*-null grandmother
168 would have been inherited by ~50% of the F2 outcross generation.
169
170 *Metabolic phenotype of WT* females.*
171 Litter sizes from WT* male and female matings were not significantly different from litter sizes
172 of true wild type matings (Fig. 3A). Furthermore, there was no difference in body weight at birth,
173 3 weeks, and 8 weeks of age between WT** and WT females (Fig. 3B), revealing that the detected
174 hepatic transcriptome changes are not the result of altered litter sizes or growth rates. Metabolic
175 phenotype analysis in 8 month-old females revealed no significant differences between WT****
176 and WT mice in body weight, fat composition, food intake, or energy expenditure (Fig. 3C).
177
178 Global serum metabolomic analysis was performed to examine the metabolic consequences of the
179 observed transcriptional dysregulation. Both WT** and WT**** female mice had abnormal
180 levels of multiple bile acids, which are synthesized in the liver (28-31) (Fig. 3D). The magnitude
181 of dysregulation was similar to that observed in KO^{KO} females (Fig. 3D), suggesting that
182 mutational ancestry is more important than the organism's genotype. These females also had
183 abnormal concentrations of various metabolic cofactors (Fig. 3E) that are associated with hepatic
184 metabolism (Fig. 3E) (32-35).

185

186 WT**** mice were metabolically challenged with 8 weeks of a high fat diet (HFD). When
187 compared with true wild type mice exposed to a HFD, WT**** females exposed to a HFD showed
188 a significant increase in multiple lipid molecules that were not dysregulated in WT**** females
189 that consumed a conventional diet, or in WT mice consuming a HFD (Fig. 3F). Thus, there were
190 latent metabolic abnormalities that could not be detected unless stressed with a HFD. The HFD
191 WT**** serum also had decreased levels of multiple other hepatic metabolites (36-38) some of
192 which were also decreased in WT HFD females although at a much lesser magnitude (Fig. 3G).
193 These findings demonstrate that the hepatic transcriptional dysregulation observed in these mice
194 has significant effects on multiple important metabolites found in the blood.

195

196 *Small RNA dysregulation.*

197 Livers of WT** females had dysfunctional expression of multiple small RNA-processing genes,
198 especially genes that regulate tRNA (*Trmt9b (39)*, *Ang (40)*, *Nsun6 (41)*, *Elac1 (42)*) (Fig. 3A) and
199 miRNA processing (*Mettl1 (43, 44)*, *Ago2 (45)*, *Exosc10*, *Syncrip (46)*) (Fig. 4A). Based on this
200 observation, in combination with the fact that gamete small RNAs can transmit non-genetically
201 inherited phenotypes in mice, we hypothesized that the observed phenotypes were driven by the
202 defective inheritance of small RNAs from the germ cells of *Khdc3* mutant ancestors. Small RNA-
203 Seq of KO^{KO} oocytes revealed dysregulation of multiple miRNAs and tRNA fragments, with
204 minimal piRNA or rRNA dysregulation (Fig. 4B). In WT**(P) oocytes, there was also abnormal
205 expression of tRNA fragments and miRNA, most of which were different small RNAs than the
206 ones dysregulated in KO^{KO} oocytes (Fig. 4C). Of note, the WT**(P) oocytes had downregulation
207 of the tRNA fragment Gly-GCC, for which expression in sperm has been associated with inherited

208 metabolic and hepatic gluconeogenesis phenotypes in offspring (1, 47, 48). There were 3 tRNA
209 fragments and 18 miRNAs that were commonly dysregulated in both KO^{KO} and WT**(P) oocytes
210 (Fig. 3D), suggesting that their abnormal expression is established in KO^{KO} oocytes and is not
211 normalized with reintroduction of a wild type *Khdc3* allele. The function of most of these
212 commonly dysregulated tsRNAs and miRNAs remains undescribed, however miR-107, which was
213 upregulated in both KO^{KO} and WT**(P) oocytes, is involved in hepatic lipid metabolism (49).
214
215 *Serum from Wild Type Mice with Ancestral History of Khdc3 Mutation is Sufficient to Alter*
216 *Hepatic Gene Expression in Offspring of Wild Type Mice*
217 Recent studies have demonstrated that circulating factors in the blood can induce intergenerational
218 phenotypes that recapitulate the effects observed in an exposure-based model (50). When serum
219 from WT* mice (genetically wild type with Khdc3-null ancestry) was injected intraperitoneally
220 into wild type females that were subsequently mated, the offspring manifested an altered hepatic
221 transcriptome (Fig. 5A-B). This observation suggests that yet-unidentified factors carried in the
222 serum are sufficient to drive the observed cross-generational changes. Of note, some genes were
223 commonly dysregulated in both this serum transfer experiment and the WT* female mice, for
224 example Cyp17a1. However, there were other genes that did not overlap between the two
225 experiments, likely because the serum transfer approach cannot reproduce the duration and
226 concentration of exposure to serum-based factors that occurs in wild type descendants of *Khdc3*
227 mutants.
228
229 **Discussion**

230 The presence of abnormal phenotypes in wild type organisms descended from mutant-carrying
231 ancestors has been described in mice and humans. This phenomenon can occur from mutations
232 that affect epigenetic phenomenon in the germ cell (6, 7, 51), but in other cases the mutation affects
233 a process that has no clear connection with heritable molecules in the germ cell, such as with
234 thyroid metabolism or type I diabetes (8, 11). In all previously described examples, the observed
235 defects disappear after one or two generations.
236
237 We find that loss-of-function mutation in *Khdc3* alters the hepatic metabolism of female wild type
238 descendants over at least 6 generations in a manner that cannot be rescued with re-introduction of
239 the wild type *Khdc3* allele. This is paralleled by abnormal levels of multiple metabolites in the
240 serum of these mice. Because there is no detectable *Khdc3* expression in the liver, we suspect that
241 the defects in WT* mice are caused by inherited molecules that affect hepatic metabolism
242 independent of the inheritance of a functional *Khdc3* gene. We expect that other metabolic tissues
243 such as the pancreas and adipose will also demonstrate evidence of metabolic dysregulation.
244
245 We utilized an outcrossing scheme to demonstrate that the observed defects persist when passed
246 only through the maternal line. In this mating scheme, 100% of the observed F2 outcrossed female
247 mice had evidence of hepatic metabolic dysregulation. This pattern of inheritance is not consistent
248 with in-cis mechanisms such as an unaccounted DNA variant, DNA methylation, or histone protein
249 modification, because in these scenarios the alleles in the *Khdc3*-null maternal grandmother would
250 be present in ~50% of the F2 outcrossed females.
251

252 We chose to examine females because of the reported fertility phenotypes in *KHDC3* human (18,
253 19) and *Khdc3* mouse female mutants (20). Human *KHDC3L*-null females are infertile, while
254 mouse *Khdc3*-null females are subfertile. The fertility defects are associated with oocyte DNA
255 methylation abnormalities that we suspect are sequelae of a more primary defect in mutant
256 organisms. There are no reports of abnormal phenotypes in *Khdc3*-null males, however our
257 detected metabolic abnormalities could affect males as well, which will be an important future
258 investigation. Furthermore, it will be important to examine how *Khdc3*-null mice transmit
259 exposure-based information across generations to affect phenotypes in non-exposed offspring, as
260 has been observed in numerous studies, most thoroughly with a HFD or stress.
261
262 We have demonstrated that *Khdc3*-null oocytes have abnormal expression of multiple miRNAs
263 and tsRNAs, some of which persist over multiple generations in WT* mice, providing a potential
264 mechanism of inheritance. Microinjection experiments using sperm RNA have demonstrated that
265 small RNAs are sufficient to drive metabolic derangements in offspring (1, 52), however the
266 maintenance of defects to the successive generation remains unexplained. The amount of RNA
267 needed for these experiments currently prevents using oocyte RNA in such an experimental
268 paradigm, because of the low total RNA yield obtained from the oocytes of a single mouse.
269
270 A recent study demonstrated that transfer of serum from a stress-exposed mouse into a non-
271 exposed mouse can recapitulate the effects observed in the exposed's offspring, suggesting serum
272 factors can modify the composition of heritable molecules in the germ cells and affect offspring
273 traits (50). Indeed, we observed that the serum from a WT* mouse is sufficient to cause hepatic
274 dysregulation when it was injected into a wild type female/mother. The observation that serum-

275 based factors can drive cross-generational hepatic transcriptome changes suggests that the
276 metabolic alterations in each generation with an ancestral history of *Khdc3* mutation drive changes
277 to heritable molecules in the oocyte, which then drive metabolic dysregulation in the next
278 generation.

279

280 One important conclusion from studies on genetic nurture is that wild type mice descended from
281 mutant ancestors should be used thoughtfully and with caution, because phenotypes can be
282 obscured that would be apparent with the use of wild type mice without any ancestral history of
283 mutation. In sum, the effect of non-inherited genetic variants on offspring phenotypes remains a
284 relatively unexplored and potentially significant contributor to traits and disease risk.

285

286 **Materials and Methods**

287 **Mice**

288 FVB/N WT (Jax 001800) mice were purchased from The Jackson Laboratory and bred in-
289 house. Frozen *Khdc3-null* sperm was obtained from the Mutant Mouse Resource and Research
290 Center (MMRRC, North Carolina) and the *Khdc*3 KO mouse was rederived. Female mice were
291 used at 8 weeks of age. In individual experiments, all animals were age-matched. All mice were
292 maintained under specific pathogen-free (SPF) conditions on a 12-hour light/dark cycle, and
293 provided food and water ad libitum. All mouse experiments were approved by, and performed in
294 accordance with, the Institutional Animal Care and Use Committee guidelines at Weill Cornell
295 Medicine.

296

297 **Mouse Genotyping**

298 As described in this study, WT mice were generated from WT parents. WT* and KO* mice were
299 generated from the mating of *Khdc3* heterozygote parents that were themselves generated from
300 mating of WT and KO^{KO} mice. KO^{KO} mice were generated from *Khdc3* KO parents. DNA was
301 extracted from tail biopsies by incubating the tails biopsies in an alkaline lysis buffer (24mM
302 NaOH and 0.2mM disodium EDTA) for 30 minutes at 95°C and then on ice for 10 minutes. A
303 neutralization buffer (40 mM Tris-HCl) was added to the samples and diluted 1:10 with water.
304 PCR to detect *Khdc3* deletion was performed with 50–200 ng of DNA using the Phire Green Hot
305 Start II DNA Polymerase Master Mix (Thermo Scientific) in the Bio-Rad T100 Thermal Cycler.
306 PCR for *Khdc3* deletion was performed using a forward primer for the wild type allele F1, a
307 separate forward primer that incorporates the deletion allele F2, and a common reverse primer R1.
308 The primers were as follows: P1: 5'-TGCCTGGGCAGGTTATTTAG-3', P2: 5'-
309 CGAGCGTCTGAAACCTCTTC-3' and P3: 5'-AGCTAGCTTGGCTGGACGTA-3'. P1 and P2
310 amplified the wild type allele and P1 and P3 amplified the *Khdc3* mutant allele (KO). The PCR
311 products were separated on a 1% agarose gel with SYBR safe DNA gel stain. Because of the
312 different sizes of the PCR products, the genotypes can be easily determined from the band patterns
313 on DNA gels.
314

315 **Liver RNA Extraction**

316 Total RNA extraction was performed on the liver of 8 week old mice using the Qiagen RNeasy
317 Lipid Tissue Mini Kit (Qiagen) according to the manufacturer's instructions. Samples were eluted
318 in 30µl nuclease-free water. Nucleic acid concentration, A260/280 and A260/230 ratios was
319 determined via NanodropD-1000 (Thermo Scientific). Extracted samples were aliquoted and
320 stored at -80°C.

321

322 **RT-PCR and quantitative RT-PCR**

323 2000ng RNA per sample was used to generate cDNA using SuperScript III First-Strand Synthesis
324 System (Invitrogen) following the manufacturer's instructions. cDNA was diluted to 1:4 in water
325 before performing qPCR using SYBR Green PCR Master Mix (Applied Biosystems). qPCR
326 reactions were performed on a QuantStudio 6 Flex Real Time PCR Instrument. Cycling conditions
327 were as follows: Initial denaturation 95°C for 3 minutes, 40 cycles of denaturation at 95°C for 15
328 seconds followed by annealing/extension at 60°C for 60 seconds. Relative expression was
329 calculated using the ΔΔCt method, using YWHAZ as the reference gene. Primers used are listed
330 in Supplemental Table 1.

331

332 **Oocyte RNA Isolation**

333 The oocytes were dissected following a published protocol with some modifications (53). Briefly,
334 the ovaries were first dissected from unstimulated 8-week-old WT and *Khdc3*-null mice and placed
335 in PBS. The ovary was dissected from surrounding para-ovarian fat and subsequently placed in a
336 35-mm culture dish with 2mL PBS and 20µl collagenase and 20µl DNase in a 37°C incubator for
337 20 minutes. Using a dissecting microscope, the oocytes were separated from granulosa cells, theca
338 cells, and stromal cells, and transferred to a petri dish with PBS using a mouth-controlled
339 micropipette. RNA was extracted from the oocytes using the PicoPure RNA Isolation kit (Thermo
340 Fisher) following the manufacturer's instructions and eluted in 20 µL of the provided elution
341 buffer.

342

343 **Liver RNA-seq Library Preparation**

344 Sequencing libraries were prepared using the Illumina TruSeq Stranded Total RNA kit according
345 to the manufacturer's protocol and sequenced to a depth of 40 million reads per sample. The
346 paired-end (PE) libraries were sequenced on Novaseq platform.
347
348 **Oocyte RNA-seq Library Preparation**
349 Sequencing libraries were prepared using the SMART-Seq v4 Ultra Low Input RNA plus
350 Nextera XT DNA Sample Preparation according to the manufacturer's protocol and sequenced to
351 a depth of 40 million reads per sample. The paired-end (PE) libraries were sequenced on
352 Novaseq platform.
353
354 **RNA-seq Bioinformatics**
355 All sequenced reads were assessed for quality using FastQC (54). Adapter trimming and filtering
356 of low-quality bases (<20) were performed using cutadapt (55). The trimmed reads were then
357 aligned with Hisat2 (56) against the mouse reference (GRCm38) genome. Per gene counts were
358 computed using htseq-count (57) (genocode M15). DESeq2 (58) bioconductor package was used
359 for normalization and differential gene expression analysis.
360
361 **Oocyte small RNA isolation**
362 Eight week old female mice were sacrificed and 30 oocytes were dissected under stereomicroscopy
363 from the ovaries of each mouse, as described above. Four separate WT, *Khdc3*-null, and WT(P)**
364 RNA samples were generated from separate mice. Total RNA was isolated using a magnet-based
365 method (ChargeSwitch Total RNA Cell Kit).
366

367 **Oocyte small RNA-Seq Library Preparation**

368 Small RNA quality and concentration was assessed using an Agilent Bioanalyzer and small RNA
369 Chip to ensure a clear small RNA population of more than 1ng. Subsequently, small RNA libraries
370 were generated and sequenced to a depth of 10 million reads per sample. Small RNA libraries were
371 generated using the NEXTFLEX Small RNA-seq Kit, which were sequenced on the Novaseq
372 platform.

373

374 **Small RNA-seq Bioinformatics**

375 Read quality was assessed using FastQC (v0.11.8), and adapter sequences were trimmed using
376 Trimmomatic (v0.39). After adapter trimming, reads were mapped sequentially to rRNA mapping
377 reads, miRbase, murine tRNAs, pachytene piRNA clusters (59), repeatmasker and Refseq using
378 Bowtie 2 alignment algorithm (v2.3.5) and totaled using Feature Counts on the Via Foundry
379 (v1.6.4) platform (60). To assess for differentially expressed small RNAs , data was loaded into R
380 Statistical Software and analyzed using the DESeq2 package (58). Differentially abundant small
381 RNAs were determined as those with a log fold change > 0.58 and P-value < 0.05.

382

383 **Serum preparation**

384 Blood was collected from the submandibular (facial) vein of mice. Approximately 400-500µl of
385 whole blood was collected from each mouse and placed in an SST amber microtainer blood
386 collection tube (BD). Blood collection tubes were placed in a 37°C incubator for 30 minutes,
387 followed by 10 minutes at 4°C. Samples were then centrifuged at 5500 RPM for 10 minutes at
388 4°C. The serum was collected from the top of the tube and stored at -80°C until needed.

389

390 **Metabolic Phenotpying**

391 Body weight, body fat composition, food intake, and energy expenditure of 8 month old female
392 mice were measured using the Promethion Core System.

393

394 **Metabolomic profiling**

395 Metabolomics profiling was conducted using ultra-high-performance liquid chromatography-
396 tandem mass-spectrometry by the metabolomics provider Metabolon Inc. (Morrisville, USA) on
397 mouse serum samples from WT, WT**(P), WT****(P) and KO^{KO} mice, as well as these mice
398 after consuming a high fat diet. The metabolomic dataset measured by Metabolon includes known
399 metabolites containing the following broad categories – amino-acids, peptides, carbohydrates,
400 energy intermediates, lipids, nucleotides, cofactors and vitamins, and xenobiotics. Statistical
401 differences were determined using unpaired t-test.

402

403 **High fat Diet**

404 Female WT and WT****(P) mice were divided into two diet groups, one group receiving a high-
405 fat diet (HFD, D12492i; Research Diets Inc., New Brunswick, NJ) and the other group received a
406 normal diet with 10% fat (D12450Ji; Research Diets Inc., New Brunswick, NJ). All mice were
407 given access to food and water *ad libitum* and were maintained on a 12:12-h light-dark artificial
408 lighting cycle. After 8 weeks of each diet, serum was collected and stored in the -80°C.

409

410 **Serum Metabolites**

411 Serum lipids were quantified using Beckman Coulter kits OSR6516, OSR6296, and OSR6295.
412 Serum proteins were precipitated using trichloroacetic acid. The pellet was then dissolved,

413 tryptic digested, desalted, and analyzed by LC-MS/MS for protein identification. The data were
414 processed by MaxQuant. MS data was searched against Uniprot mouse protein database.
415
416 **Serum Transfer**
417 Serum was obtained from WT and WT* (WT females descended from Khdc3-null ancestors), as
418 described above. Pooled WT serum was injected intraperitoneally into 3-month old female WT
419 (n=2) and WT* (n=2) mice. Similarly, pooled WT* serum was injected IP into female WT (n=2)
420 and WT* (n=2) mice. IP injections consisted of 200µl pooled serum every 12 hours for 3 doses
421 (each mouse received a total of 600µl injected serum). The female WT and WT* mice were
422 subsequently mated with a WT male 24 hours later. Livers from female mice of each offspring
423 were dissected at 1 month of life. RNA was extracted and RNA sequencing was performed on
424 the samples, as described above.
425
426 **Statistical Analysis and data visualization**
427 Gene ontology performed with WebGestalt (https://www.webgestalt.org/) using KEGG analysis.
428 Volcano plots generated with ggVolcanoR (https://ggvolcanor.erc.monash.edu). Venn diagrams
429 generated with InteractiVenn (http://www.interactivenn.net/). Scatter plots were generated with
430 Prism 9.2.0. The manuscript was written using Microsoft Word v16.66.1. Figures were
431 assembled on Microsoft PowerPoint v16.66.1
432
433 **Data Availability:** All RNA-Seq and small RNA-Seq data are available in the NCBI GEO
434 database, accession numbers GSE281631 (oocyte RNA-Seq, Figure 1), GSE 282184 (liver RNA-
435 Seq, Fig. 1), GSE283285 (liver RNA-Seq, Fig. 2), GSE288429 (F2 outcross liver RNA-Seq,

Figure 2), GSE 287350 (oocyte small RNA-Seq, Figure 4), and GSE288414 (serum transfer RNA-Seq, Figure 5).

Acknowledgements

This work was supported by the Young Investigator Award (LS) at Weill Cornell Medicine, Pediatric Scientist Development Program under the National Institute of Child Health under award number K12HD000850 (SC), Friedman Family Clinical Scholar Award (MSR), and National Institute of Child Health and Human Development (NICHD) of the National Institutes of Health under award number P50HD104454 (MSR).

Author Contributions

L.S. and M.S.R. conceived and planned the experiments. L.S., S.C., N.H., H.F., K.P., and M.S.R carried out the experiments. U.B., N.T., J.G., and C.C. performed bioinformatic analysis of the RNA-Seq and small RNA-Seq data. L.S. and M.S.R. prepared the manuscript. All authors provided critical feedback and contributed to shaping the research, analysis, and manuscript.

References

1. Q. Chen *et al.*, Sperm tsRNAs contribute to intergenerational inheritance of an acquired metabolic disorder. *Science* **351**, 397-400 (2016).
2. U. Sharma, Paternal Contributions to Offspring Health: Role of Sperm Small RNAs in Intergenerational Transmission of Epigenetic Information. *Front Cell Dev Biol* **7**, 215 (2019).
3. L. O. Bygren, G. Kaati, S. Edvinsson, Longevity determined by paternal ancestors' nutrition during their slow growth period. *Acta Biotheor* **49**, 53-59 (2001).
4. G. Kaati, L. O. Bygren, S. Edvinsson, Cardiovascular and diabetes mortality determined by nutrition during parents' and grandparents' slow growth period. *Eur J Hum Genet* **10**, 682-688 (2002).
5. K. Gapp *et al.*, Implication of sperm RNAs in transgenerational inheritance of the effects of early trauma in mice. *Nat Neurosci* **17**, 667-669 (2014).

465 6. D. Carouge *et al.*, Parent-of-origin effects of A1CF and AGO2 on testicular germ-cell
466 tumors, testicular abnormalities, and fertilization bias. *Proc Natl Acad Sci U S A* **113**,
467 E5425-5433 (2016).
468 7. M. Y. Lam, J. D. Heaney, K. K. Youngren, J. H. Kawasoe, J. H. Nadeau, Trans-generational
469 epistasis between Dnd1Ter and other modifier genes controls susceptibility to testicular
470 germ cell tumors. *Hum Mol Genet* **16**, 2233-2240 (2007).
471 8. J. Anselmo, N. H. Scherberg, A. M. Dumitrescu, S. Refetoff, Reduced Sensitivity to Thyroid
472 Hormone as a Transgenerational Epigenetic Marker Transmitted Along the Human Male
473 Line. *Thyroid* **29**, 778-782 (2019).
474 9. S. N. Yazbek, S. H. Spiezio, J. H. Nadeau, D. A. Buchner, Ancestral paternal genotype
475 controls body weight and food intake for multiple generations. *Hum Mol Genet* **19**, 4134-
476 4144 (2010).
477 10. V. R. Nelson, S. H. Spiezio, J. H. Nadeau, Transgenerational genetic effects of the paternal
478 Y chromosome on daughters' phenotypes. *Epigenomics* **2**, 513-521 (2010).
479 11. S. T. Bennett *et al.*, Insulin VNTR allele-specific effect in type 1 diabetes depends on
480 identity of untransmitted paternal allele. The IMDIAB Group. *Nat Genet* **17**, 350-352
481 (1997).
482 12. N. Padmanabhan *et al.*, Mutation in folate metabolism causes epigenetic instability and
483 transgenerational effects on development. *Cell* **155**, 81-93 (2013).
484 13. A. Kong *et al.*, The nature of nurture: Effects of parental genotypes. *Science* **359**, 424-428
485 (2018).
486 14. I. R. Adams, R. R. Meehan, From paramutation to paradigm. *PLoS Genet* **9**, e1003537
487 (2013).
488 15. S. Yuan, D. Oliver, A. Schuster, H. Zheng, W. Yan, Breeding scheme and maternal small
489 RNAs affect the efficiency of transgenerational inheritance of a paramutation in mice. *Sci*
490 *Rep* **5**, 9266 (2015).
491 16. Y. Zhang *et al.*, Dnmt2 mediates intergenerational transmission of paternally acquired
492 metabolic disorders through sperm small non-coding RNAs. *Nat Cell Biol* **20**, 535-540
493 (2018).
494 17. P. Huypens *et al.*, Epigenetic germline inheritance of diet-induced obesity and insulin
495 resistance. *Nat Genet* **48**, 497-499 (2016).
496 18. H. Demond *et al.*, A KHDC3L mutation resulting in recurrent hydatidiform mole causes
497 genome-wide DNA methylation loss in oocytes and persistent imprinting defects post-
498 fertilisation. *Genome Med* **11**, 84 (2019).
499 19. D. Bebbere, L. Masala, D. F. Albertini, S. Ledda, The subcortical maternal complex:
500 multiple functions for one biological structure? *J Assist Reprod Genet* **33**, 1431-1438
501 (2016).
502 20. P. Zheng, J. Dean, Role of Filia, a maternal effect gene, in maintaining euploidy during
503 cleavage-stage mouse embryogenesis. *Proc Natl Acad Sci U S A* **106**, 7473-7478 (2009).
504 21. Y. Wang, T. Nakajima, F. J. Gonzalez, N. Tanaka, PPARs as Metabolic Regulators in the
505 Liver: Lessons from Liver-Specific PPAR-Null Mice. *Int J Mol Sci* **21** (2020).
506 22. P. R. Nagareddy, S. K. Noothi, M. C. Flynn, A. J. Murphy, It's reticulated: the liver at the
507 heart of atherosclerosis. *J Endocrinol* **238**, R1-R11 (2018).
508 23. A. Czumaj *et al.*, The Pathophysiological Role of CoA. *Int J Mol Sci* **21** (2020).

24. H. S. Han, G. Kang, J. S. Kim, B. H. Choi, S. H. Koo, Regulation of glucose metabolism from a liver-centric perspective. *Exp Mol Med* **48**, e218 (2016).
25. A. Milona *et al.*, Steroidogenic control of liver metabolism through a nuclear receptor-network. *Mol Metab* **30**, 221-229 (2019).
26. T. T. Wu *et al.*, Mutated CYP17A1 promotes atherosclerosis and early-onset coronary artery disease. *Cell Commun Signal* **21**, 155 (2023).
27. P. Nguyen *et al.*, Liver lipid metabolism. *J Anim Physiol Anim Nutr (Berl)* **92**, 272-283 (2008).
28. J. Y. Chiang, Bile acid metabolism and signaling. *Compr Physiol* **3**, 1191-1212 (2013).
29. S. A. Ahmed *et al.*, Xanthosine, a purine glycoside mediates hepatic glucose homeostasis through inhibition of gluconeogenesis and activation of glycogenesis via regulating the AMPK/ FoxO1/AKT/GSK3β signaling cascade. *Chem Biol Interact* **371**, 110347 (2023).
30. M. Kusaczuk, Tauroursodeoxycholate-Bile Acid with Chaperoning Activity: Molecular and Cellular Effects and Therapeutic Perspectives. *Cells* **8** (2019).
31. F. Brial *et al.*, The Natural Metabolite 4-Cresol Improves Glucose Homeostasis and Enhances β-Cell Function. *Cell Rep* **30**, 2306-2320.e2305 (2020).
32. J. E. Klaunig, X. Li, Z. Wang, Role of xenobiotics in the induction and progression of fatty liver disease. *Toxicol Res (Camb)* **7**, 664-680 (2018).
33. I. Lahdou *et al.*, Increased serum levels of quinolinic acid indicate enhanced severity of hepatic dysfunction in patients with liver cirrhosis. *Hum Immunol* **74**, 60-66 (2013).
34. A. Sambeat *et al.*, Endogenous nicotinamide riboside metabolism protects against diet-induced liver damage. *Nat Commun* **10**, 4291 (2019).
35. G. Liang *et al.*, Nicotinamide N-methyltransferase and liver diseases. *Genes Dis* **10**, 1883-1893 (2023).
36. M. H. Kim *et al.*, Daidzein supplementation prevents non-alcoholic fatty liver disease through alternation of hepatic gene expression profiles and adipocyte metabolism. *Int J Obes (Lond)* **35**, 1019-1030 (2011).
37. L. Seidemann, A. Krüger, V. Kegel-Hübner, D. Seehofer, G. Damm, Influence of Genistein on Hepatic Lipid Metabolism in an In Vitro Model of Hepatic Steatosis. *Molecules* **26** (2021).
38. T. Kose, J. Moreno-Fernandez, M. Vera-Aviles, P. A. Sharp, G. O. Latunde-Dada, Ferulic acid protects HepG2 cells and mouse liver from iron-induced damage. *Biochem Biophys Rep* **35**, 101521 (2023).
39. P. C. Dedon, T. J. Begley, Dysfunctional tRNA reprogramming and codon-biased translation in cancer. *Trends Mol Med* **28**, 964-978 (2022).
40. P. Ivanov, M. M. Emara, J. Villen, S. P. Gygi, P. Anderson, Angiogenin-induced tRNA fragments inhibit translation initiation. *Mol Cell* **43**, 613-623 (2011).
41. S. Haag *et al.*, NSUN6 is a human RNA methyltransferase that catalyzes formation of m5C72 in specific tRNAs. *RNA* **21**, 1532-1543 (2015).
42. M. C. J. Yip, S. Savickas, S. P. Gygi, S. Shao, ELAC1 Repairs tRNAs Cleaved during Ribosome-Associated Quality Control. *Cell Rep* **30**, 2106-2114.e2105 (2020).
43. R. García-Vílchez *et al.*, METTL1 promotes tumorigenesis through tRNA-derived fragment biogenesis in prostate cancer. *Mol Cancer* **22**, 119 (2023).

552 44. L. Pandolfini *et al.*, METTL1 Promotes let-7 MicroRNA Processing via m7G Methylation.
553 *Mol Cell* **74**, 1278-1290.e1279 (2019).
554 45. J. O'Brien, H. Hayder, Y. Zayed, C. Peng, Overview of MicroRNA Biogenesis, Mechanisms
555 of Actions, and Circulation. *Front Endocrinol (Lausanne)* **9**, 402 (2018).
556 46. L. Santangelo *et al.*, The RNA-Binding Protein SYNCRIP Is a Component of the Hepatocyte
557 Exosomal Machinery Controlling MicroRNA Sorting. *Cell Rep* **17**, 799-808 (2016).
558 47. B. Wang *et al.*, Paternal High-Fat Diet Altered Sperm 5'tsRNA-Gly-GCC Is Associated With
559 Enhanced Gluconeogenesis in the Offspring. *Front Mol Biosci* **9**, 857875 (2022).
560 48. U. Sharma *et al.*, Biogenesis and function of tRNA fragments during sperm maturation and
561 fertilization in mammals. *Science* **351**, 391-396 (2016).
562 49. H. Bhatia, G. Verma, M. Datta, miR-107 orchestrates ER stress induction and lipid
563 accumulation by post-transcriptional regulation of fatty acid synthase in hepatocytes.
564 *Biochim Biophys Acta* **1839**, 334-343 (2014).
565 50. G. van Steenwyk *et al.*, Involvement of circulating factors in the transmission of paternal
566 experiences through the germline. *EMBO J* **39**, e104579 (2020).
567 51. B. J. Lesch *et al.*, Intergenerational epigenetic inheritance of cancer susceptibility in
568 mammals. *Elife* **8** (2019).
569 52. Q. Chen, W. Yan, E. Duan, Epigenetic inheritance of acquired traits through sperm RNAs
570 and sperm RNA modifications. *Nat Rev Genet* **17**, 733-743 (2016).
571 53. S. El-Hayek, Q. Yang, L. Abbassi, G. FitzHarris, H. J. Clarke, Mammalian Oocytes Locally
572 Remodel Follicular Architecture to Provide the Foundation for Germline-Soma
573 Communication. *Curr Biol* **28**, 1124-1131.e1123 (2018).
574 54. S. Andrews (2010) *FastQC: a quality control tool for high throughput sequence data*. p
575 *Available online at:* http://www.bioinformatics.babraham.ac.uk/projects/fastqc.
576 55. M. Martin, Cutadapt removes adapter sequences from high-throughput sequencing
577 reads. *EMBnet J* (2011).
578 56. D. Kim, J. M. Paggi, C. Park, C. Bennett, S. L. Salzberg, Graph-based genome alignment and
579 genotyping with HISAT2 and HISAT-genotype. *Nat Biotechnol* **37**, 907-915 (2019).
580 57. S. Anders, P. T. Pyl, W. Huber, HTSeq--a Python framework to work with high-throughput
581 sequencing data. *Bioinformatics* **31**, 166-169 (2015).
582 58. M. I. Love, W. Huber, S. Anders, Moderated estimation of fold change and dispersion for
583 RNA-seq data with DESeq2. *Genome Biol* **15**, 550 (2014).
584 59. X. Z. Li *et al.*, An ancient transcription factor initiates the burst of piRNA production during
585 early meiosis in mouse testes. *Mol Cell* **50**, 67-81 (2013).
586 60. O. Yukselen, O. Turkyilmaz, A. R. Ozturk, M. Garber, A. Kucukural, DolphinNext: a
587 distributed data processing platform for high throughput genomics. *BMC Genomics* **21**,
588 310 (2020).
589

590

591 **Figures**

592 **Figure 1**

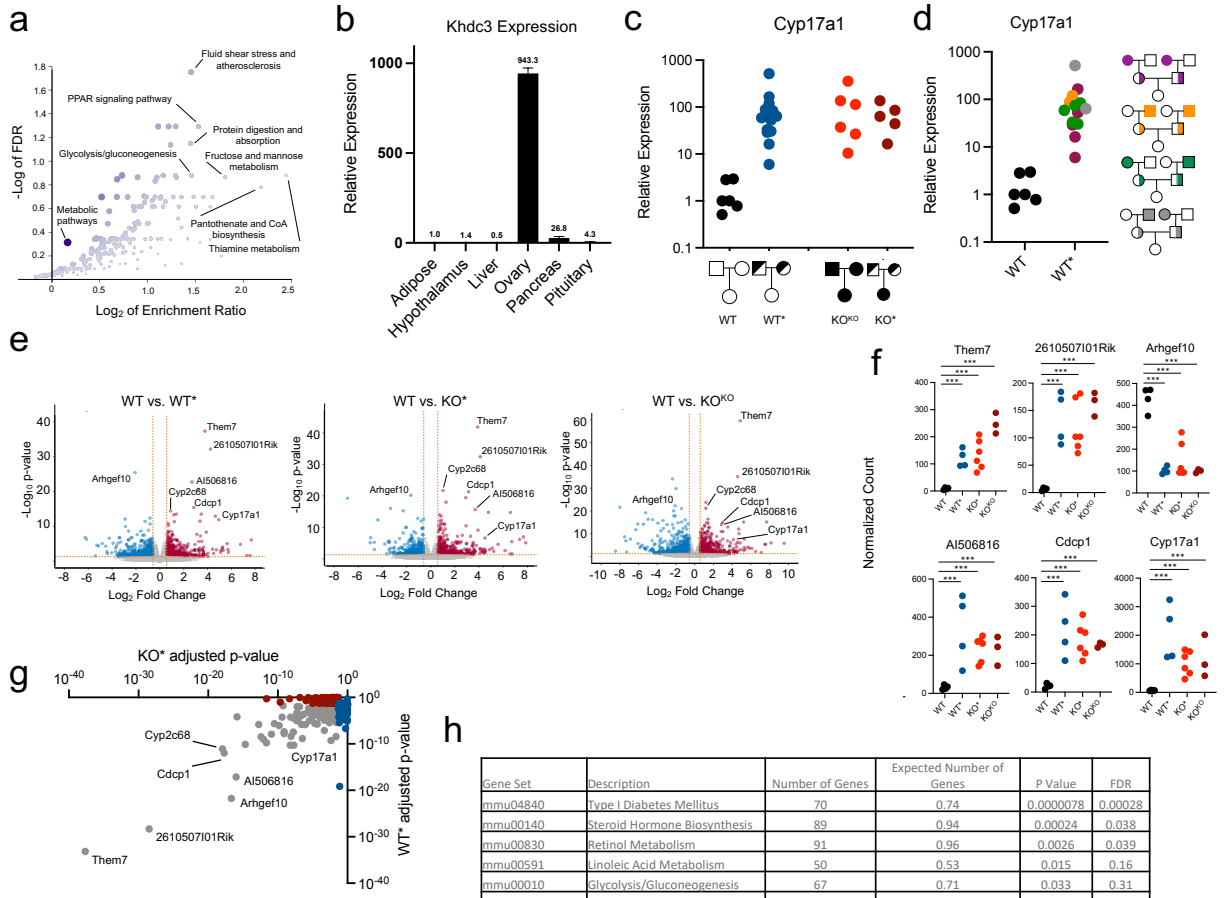

Gene Set	Description	Number of Genes	Expected Number of Genes	P Value	FDR
mmu04840	Type I Diabetes Mellitus	70	0.74	0.0000078	0.00028
mmu00140	Steroid Hormone Biosynthesis	89	0.94	0.00024	0.038
mmu00830	Retinol Metabolism	91	0.96	0.0026	0.039
mmu00591	Linoleic Acid Metabolism	50	0.53	0.015	0.16
mmu00010	Glycolysis/Gluconeogenesis	67	0.71	0.033	0.31
mmu00590	Arachidonic Acid Metabolism	89	0.94	0.067	0.57
mmu00600	Sphingolipid Metabolism	48	0.5	0.09	0.71

593

594 **Figure 1. Female mice with an ancestral history of Khdc3 mutation manifest hepatic**

595 **transcriptional dysregulation that is independent of genotype.**

596 **(a)** Gene ontology scatterplot for dysregulated genes in *Khdc3*-null oocytes, based on RNA-Seq.

597 The y-axis represents −log FDR (false discovery rate) and the x-axis represents $\log_2$ enrichment

598 ratio. Dysregulation of genes important in lipid and carbohydrate metabolism are highlighted. **(b)**

599 Murine expression of *Khdc3* in various tissues, detected by qPCR (N=3). **(c)** Relative mRNA

600 expression of *Cyp17a1* in the livers of WT, WT*, KO^{KO}, and KO* mice measured by qPCR. Each

601 dot represents an individual mouse. **(d)** Relative mRNA expression of *Cyp17a1* in the livers of

602 WT* female mice generated from various male and female *Khdc3*-null grandparents measured by

603 qPCR. **(e)** Volcano plots depicting differentially expressed genes identified by RNA-seq in the
604 livers of WT vs. WT*, KO* and KO^{KO} mice, respectively (N=4-6). Red dots represent upregulated
605 genes in WT*, KO* and KO^{KO} mice while blue dots represent genes that were downregulated in
606 WT*, KO* and KO^{KO} mice. The x-axis shows $\log_2$ fold change values, and the y-axis denotes
607 $-\log_{10}$ p-values. **(f)** Dot plots of common dysregulated liver genes amongst the WT*, KO*, and
608 KO^{KO} mice compared to WT mice; ***p-adjusted $< 1 \times 10^{-5}$. **(g)** Dot plot of the significantly
609 dysregulated genes in KO* livers (x-axis) versus WT* livers (y-axis), based on adjusted p-
610 value. Red dots reveal significantly dysregulated genes in KO* mice, blue dots reveal significantly
611 dysregulated genes in WT* mice, and grey dots represent commonly significantly dysregulated
612 genes in both KO* and WT* mice. **(h)** Gene ontology of the most common dysregulated genes
613 identified in the livers of both WT* and KO* revealed abnormalities in pathways critical for lipid
614 and glucose metabolism.

615 **Figure 2**

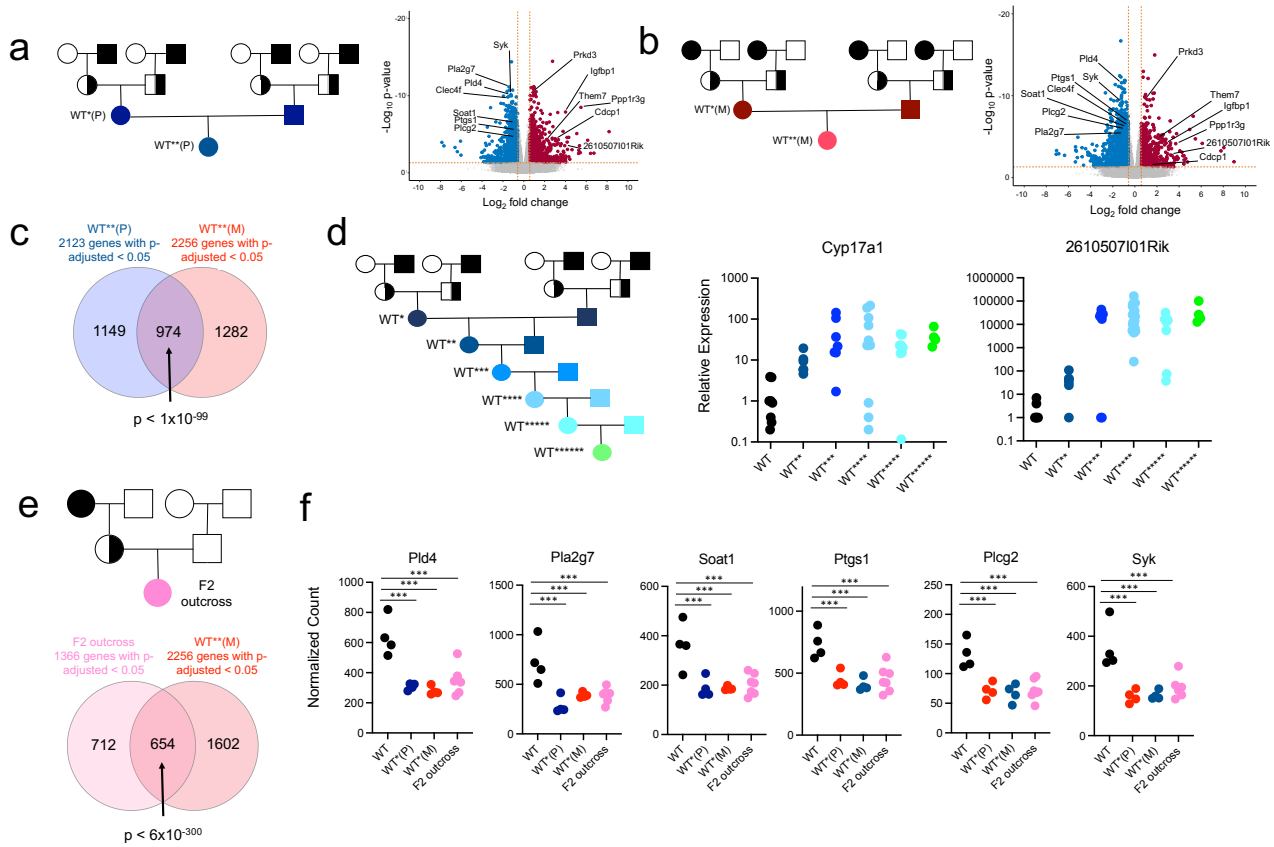

616

617 **Figure 2. WT* defects persist over multiple generations and can be passed through the**

618 **maternal and paternal ancestral lines. (a)** Schematic of experimental mating to form WT**(P)

619 mice. *Khdc3*-null mice are represented by black filled shapes, WT mice represented by white filled

620 shapes, and *Khdc3*-heterozygote mice represented by half-filled black shapes. Volcano plot

621 displaying dysregulated genes in the livers of WT**(P) mice compared to WT mice (N=4). Red

622 dots represent upregulated genes and blue dots represent downregulated genes in the WT**(P)

623 mice. **(b)** Schematic of experimental mating to form WT**(M) mice. Volcano plot displaying

624 dysregulated genes in the livers of WT**(M) mice compared to WT mice (N=4). Red dots

625 represent upregulated genes and blue dots represent downregulated genes in the WT**(M) mice.

626 **(c)** Venn diagram representing the number of significantly dysregulated liver genes of WT**(P)

627 and WT**(M) female mice compared to WT mice. **(d)** Pedigree schematic representing mating of

628 WT*(P) male and female mice over successive generations to form WT******(P) mice. Dot plots
629 represent relative liver mRNA expression of *Cyp17a1* and *2610507I01Rik* of the 2nd through 7th
630 generation WT female mice descended from male *Khdc3*-null mice as measured by qPCR. **(e)**
631 Pedigree schematic representing creation of a F2 outcross WT female from the mating of a female
632 *Khdc3*-null female and WT male and subsequent F1 generation *Khdc3*-heterozygote female with
633 WT male. Venn diagram depicting the overlap of commonly dysregulated genes in the livers of
634 F2 outcross WT and WT**(M) female mice compared to WT mice (N=4-7). **(f)** Dot plots
635 representing liver gene dysregulation amongst WT, WT*(P), WT*(M), and F2 outcross WT
636 female mice. ***$p < 1 \times 10^{-5}$.
637

638 **Figure 3**

639

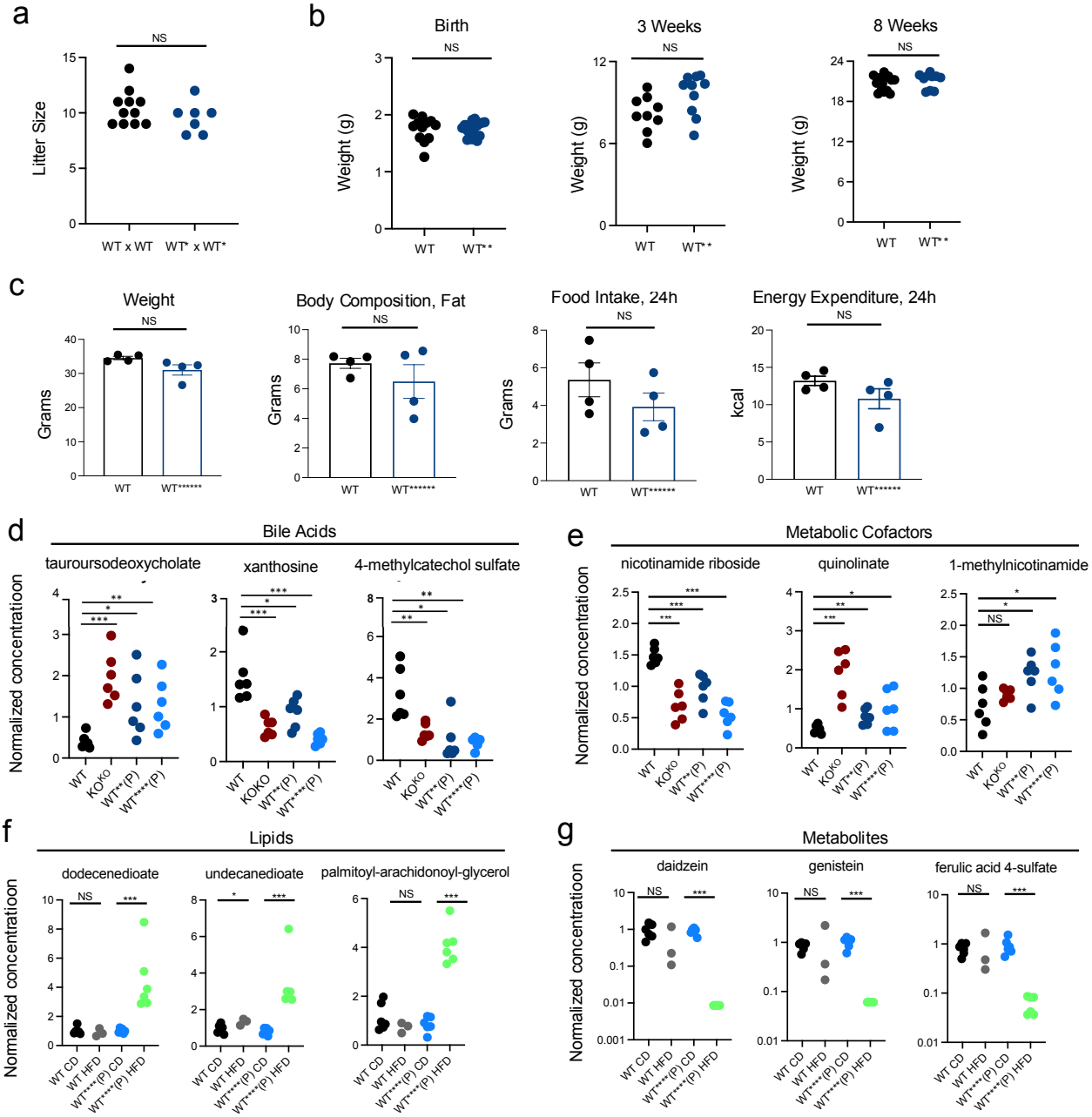

640

641 **Figure 3. Wild type mice with ancestral history of *Khdc3* mutation have dysregulation of**

642 **multiple hepatically-metabolized molecule in the serum. (a)** Litter sizes in wild type (WT x

643 WT) and WT* (WT* x WT*) matings. **(b)** Weights of WT** pups at birth, 3 weeks, and 8 weeks.

644 **(c)** Metabolic phenotype of WT****** females at 8 months of age, including weight, fat

645 composition, food intake, and energy expenditure. **(d-e)** Dot plots revealing concentration of bile

646 acids and metabolic cofactors in KO^{KO}, WT**(P), and WT****(P) female mice compared to WT
647 mice. **(f)** Dot plots revealing metabolic cofactors in WT****(P) female mice exposed to a HFD
648 compared to WT**** mice fed a conventional diet and WT mice fed a HFD. **(g)** Dot plots
649 revealing metabolites in WT****(P) female mice exposed to a HFD compared to WT**** mice
650 fed a conventional diet and WT mice fed a HFD. *$p < 0.05$, **$p < 0.005$, ***$p < 0.0005$.

651 **Figure 4**

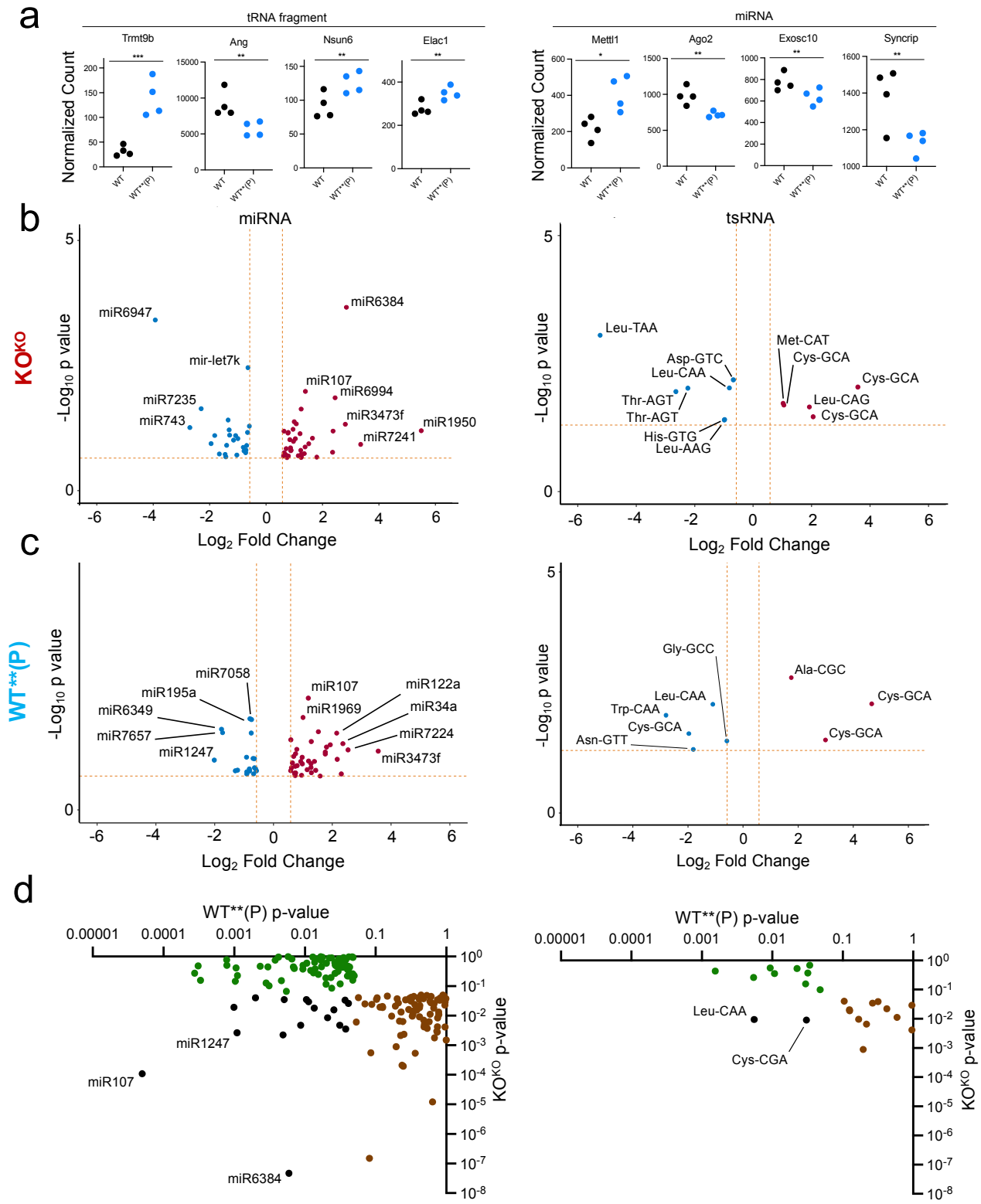

652

653 **Figure 4. Oocytes of KOKO and WT**(P) mice have dysregulated expression of multiple**
654 **miRNAs and tsRNAs. (a)** Dot plots representing dysfunctional expression of small RNA-
655 processing genes of the livers of WT**(P) mice as measured in RNA-seq**. (b)** Volcano plots
656 depicting differentially expressed miRNAs and tRNA fragments in KO^{KO} oocytes compared to
657 WT oocytes. Red dots represent upregulated small RNAs, and blue dots represent downregulated
658 small RNAs (N=4). **(c)** Volcano plots depicting differentially expressed miRNAs and tRNA
659 fragments in WT**(P) oocytes compared to WT oocytes. Red dots represent upregulated small
660 RNAs, and blue dots represent downregulated small RNAs (N=4). **(d)** Scatterplot of the most
661 significantly dysregulated small RNAs of WT**(P) oocytes (x-axis) versus KO^{KO} oocytes (y-
662 axis), based on p-value. Green dots reveal dysregulated miRNAs and tRNA fragments in WT**(P)
663 oocytes, brown dots reveal dysregulated miRNAs and tRNA fragments in KO^{KO} oocytes, and
664 black dots represent commonly dysregulated small RNAs in both WT**(P) and KO^{KO} oocytes.
665
666
667
668
669
670
671
672
673
674
675
676

677 **Figure 5**

678

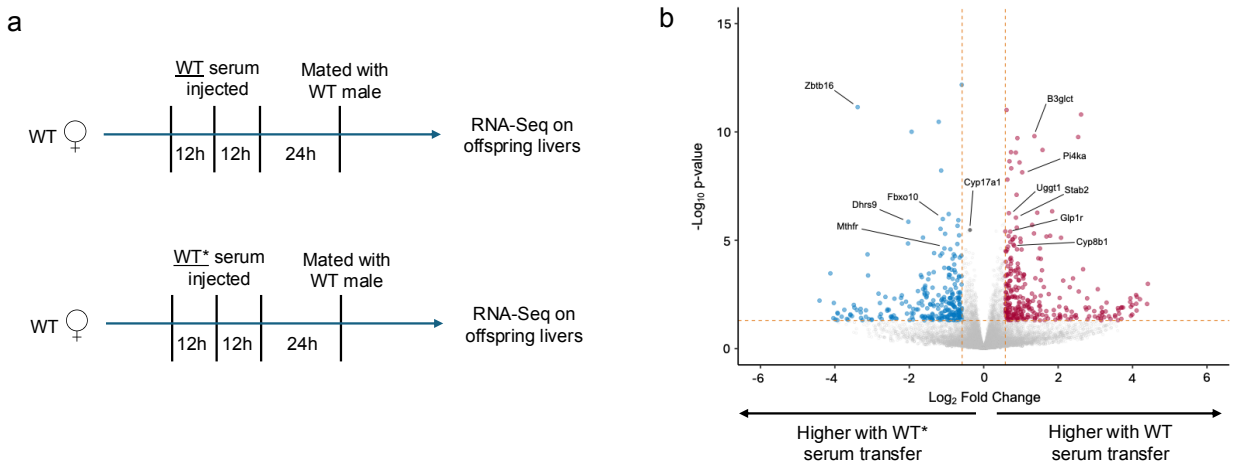

679

680

681 Figure 5. Injection of serum from KO mice in WT females is sufficient to cause transcriptional

682 dysregulation in WT offspring. (a) Schematic of serum transfer experiment. (d) Volcano plot

683 depicting differentially expressed genes in the wild type offspring born to mothers who received

684 injection with either WT or KO serum. *$p < 0.05$, **$p < 0.005$, ***$p < 0.0005$.

685

686

687

688

689

690

691

692

693

694

695

696 **Additional Information**

697 Supplementary Information is available for this paper.

698 **<u>Supplemental Material</u>**

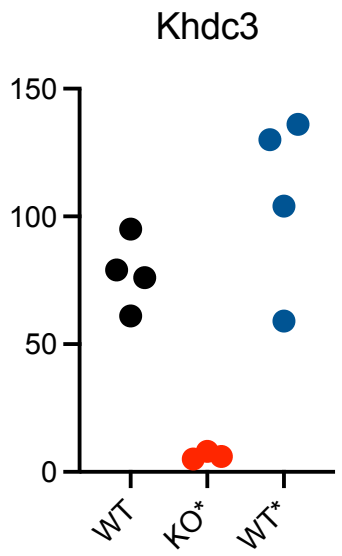

699

700 **Supplemental Figure 1.**

701 *Khdc3* expression in ovaries of WT, KO*, and WT* mice, from RNA-Seq.

702

703 **Supplemental Table 1: Primer sequences used for qPCR**

Gene	Primer Sequence
YWHAZ	Forward primer: 5' CAGAAGACGGAAGGTGCTGAGA 3' Reverse primer: 5' CTTTCTGGTTGCGAAGCATTGGG 3'
Cyp17a1	Forward primer: 5'ACTGCAGTGATTGTCGGTCA 3' Reverse primer: 5' CTAGAGTCACCATCTGGGGC 3'
2610507I01Rik	Forward primer: 5' GGATCTGATAGTCGCCCGTG 3' Reverse primer: 5' TCGCAAGAGTTCCCTGCTTT 3'

704